Optimization of A Bidirectional Boost Converter for Nanogrid Applications

Rand AL Mdanat* , Sarah Saeed* , Ramy Georgious* , Jorge Garcia* , Francesco Iannuzzo†
* Lemur Research Group, Electrical Engineering Dept., University of Oviedo, Gijon, Spain
† REPEC Group, AAU Energy Dept., University of Aalborg, Aalborg , Denemark

***Abstract*—The electrical distribution system is undergoing a transformation from centralized to distributed generation, particularly in rural areas with limited grid access. This change is supported by advancements in key technologies, including distributed resources, renewable generators, electricity storage systems, and power electronic converters which enable the efficient and reliable integration of all energy systems within the nanogrid. Given the importance of the DC/DC converter in a nanogrid and the increasing requirements, optimizing its design is essential for improving the nanogrid's overall performance.**

This paper proposes an optimization method for a bidirectional boost converter that optimizes cost and efficiency as a function of switching frequency, current ripple, and other parameters. The optimization is performed using a genetic algorithm widely used in power electronics design optimization problems. Analytical models for cost and power losses are used to solve the optimization. Several solutions to the optimization problem are presented, dependent on the weight of the objective function, which can be customized to suit the user's preferences.

***Index Terms*—nanogrid, optimization, genetic algorithm, boost converter, modeling**

I. Introduction

The electrical distribution system has shifted from centralized to distributed generation, benefiting rural areas with limited grid access. This paradigm involves the implementation of microgrids and nanogrids, which are autonomous electrical sub-networks that can function in isolated mode from the main grid [1]–[5]. Key technologies for this shift include the development of distributed resources, renewable generators like wind and solar, electricity storage systems, and power electronic converters (PEC). These PEC enable effective, reliable, and efficient interconnection of all the energy systems within the nanogrid.

Various power converter topologies and algorithms for nanogrids are proposed in the literature, with a focus on hardware and control [5]. However, the critical role of the PEC in the nanogrid system and the rising demand for these PEC open a field of research that seeks to optimize the design of these converters to ensure satisfactory performance, based on different objective functions (efficiency, cost, performance, size, etc.) [6]–[11]. For instance, in some designs, weight and cost may be critical, whereas, in others, efficiency can be left unconstrained within a reasonable range. On the other hand, efficiency and cost are efficiency and cost are more important other applications. These objectives can be stated in terms of a multi-objective function with weighting values or a constrained optimization with one attribute optimized subject to a constraint on another [12]. In nanogrid applications, the primary attention is directed toward maximizing efficiency and minimizing costs while balancing conflicting objectives.

This work has been partially funded from the EU H2020 R&I Program under grant agreement 864459 (Project "TALENT"), and through ERFD Structural Funds. This wok has been partially supported by PID2019-111051RB-100 (Project "B2B- Energy"), and the government of Principality of Asturias (FICYT), under Grant FC-GRUPIN-IDI/2018/000241 and Severo Ochoa research grant PF-BP19-078.

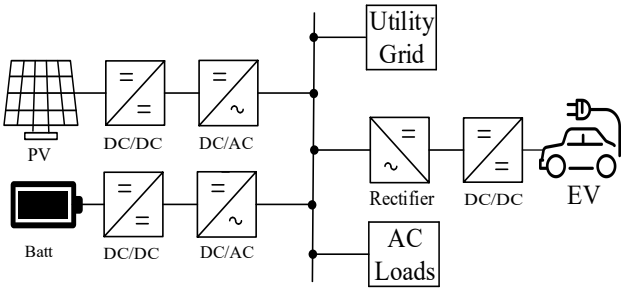

Fig. 1: Nanogrid system architecture

Generally, solar PV and battery storage, both of which are DC, are the most prevalent nanogrid constituents. DC/DC converter is the gateway that connects them either to the DC link or to the DC/AC converter and then to the AC link. Fig.1 represents the Nanogrid system architecture. Therefore, it is a critical device of the nanogrid system, and ensuring its best performance by optimizing the design will improve the total performance of the nanogrid system.

The first steps in optimization problems are to specify the design objectives and operating conditions, after that, create the models for the objective functions, and finally, choose the right optimization tool to solve the problem. The final goal of the research is to optimize the design of a DC/DC converter for nanogrid applications, by creating a global optimization tool that translates all the objective functions into a common framework. Therefore, the final output of the optimization tool will be in a single unit, which is the economical unit (cost in euros €). This cost is not only the cost related to design, manufacturing, commissioning, and operation costs (efficiency, tariff, etc.), but also the ones related to size, weight, operating lifetime, and, in general, any relevant operation parameter. However, in this article, the first approach of the work is presented which is optimizing the efficiency and the cost of a DC/DC converter in a nanogrid application, and for future work, other objectives will be added such as reliability,

size, and weight. Note that at this stage of the work, the optimization is done at the rated power of the converter, later on, the optimization algorithm will be extended to include the mission profile.

Power converter design optimization is complex because the design of a converter involves many factors such as topology design, parameter selection, semiconductor and inductor modeling, and power loss calculation. As a result, designing power converters requires a lot of computational work and resources. However, Artificial Intelligence (AI) techniques have lately become the most potent and advanced frontier in power electronics, and they are expected to have a significant impact on the upcoming generation of power electronics [13].

In section II, an overview of the applications of AI is discussed. Section III, the multi-objective optimization procedure is explained. In section IV, the design specifications, and the design constraints are presented. Descriptive models of the components used in this topology are given in section V. Finally, the optimal design of the converter is presented in section VI.

II. Overview of AI Application in Power Electronics

AI can be defined as the ability of the machine to operate intelligently and independently, which is capable of humanlike learning and reasoning. Power electronics control is a leading research area for AI implementation in power electronics, while design and maintenance applications have been increasing since 2007. AI functions in power electronics include data exploration, classification, regression, and optimization, with optimization and regression being the primary tasks [7], [13]–[15].

AI techniques in power electronics are sorted into an expert system, fuzzy logic, metaheuristic methods, and machine learning [13], [15]. Among these, metaheuristic methods are popular for optimization functions as they provide a general, scalable solution that requires less specialized expertise. Metaheuristic methods can be categorized into trajectory-based (such as the tabu search method [16] or the simulated annealing method [17]), and population-based techniques. Population-based methods like genetic algorithms(GA) [18], particle swarm optimization (PSO) [12], [19] and ant colony optimization (ACO) algorithm [20] are more efficient than trajectory-based methods in terms of convergence speed and capacity for global searching, making them suitable for large-scale optimization projects. The most commonly used metaheuristic techniques in power electronics optimization are genetic algorithm and particle swarm optimization, chosen based on the application.

The design specifications for a power converter may be in continuous space or discrete space, resulting in a mixed-integer optimization problem. Continuous design parameters include switching frequency, current ripple, and voltage ripple, while discrete design parameters include transistors and inductor design. In this research, GA is chosen over PSO and ACO to solve the optimization problem. This is because GA excels at nonlinear and mixed-integer optimization, has a fast convergence rate, and is capable of handling multi-objective optimization problems [21]. While PSO is suitable for continuous optimization and ACO for discrete optimization. Furthermore, GA continues to evolve and has an improved variant, the nondominated sorting GA II (NSGA II) [6], [22]–[24], specifically for multi-objective optimization tasks.

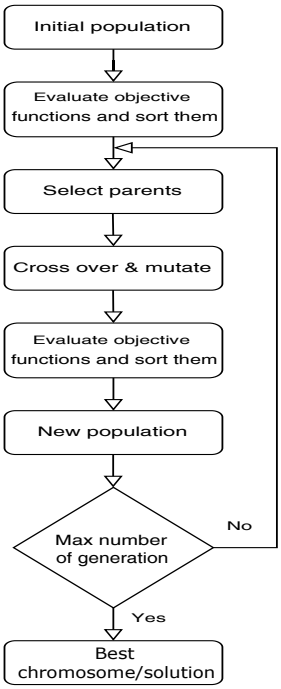

Fig. 2: Structure of GA

To solve the multi-objective optimization design for the boost converter, GA is used as a population-based method, where each individual in the population represents a distinct design through a ”gene string” that symbolizes the possible value of variable parameters determining the converter design [6], [18]. The structure of the GA is shown in Fig. 2.

Nevertheless, in future work, machine learning techniques can be joined with GA for better and faster optimization results, similar to what has been applied in [21] where they used machine learning to build data-driven models and GA to optimize the converter, as well in [7] they have merged machine learning techniques with PSO for optimization.

III. Optimization Procedure

A wide variety of power electronic converters topologies has been proposed for nanogrid application. This paper begins by selecting a DC/DC bidirectional boost topology where the work can be extended to any other topology. However, the novelty of this work is creating an optimization tool that will be able to optimize many objective functions and translate the output to one common framework which is an economical unit (€), it makes it better and easier to evaluate and compare between the solutions. This tool will give the user the freedom to weigh the objective functions depending on his preference.

The tool will be able to give the user commercial components needed for his design.

As previously stated, converter design has major concerns such as efficiency, size, weight, cost, and reliability [8], [11]. These quantities are affected by multiple design and operation parameters, such as the choice of power and control components (power semiconductors, reactive elements design) and subsystems (digital controller, gate drivers, sensors and signal conditioning sub-circuits, etc.), the control parameters (switching frequency, design of dynamic control parameters, etc.), the load and demand profiles (mission profile, environmental conditions, etc.) [25], [26], and so on.

To improve performance, multiple design objectives are considered together, requiring multi-objective optimization. Such optimization problems involve conflicting design objectives where improving one lead to the decrease of another. Pareto-front optimal solutions, rather than a unique global solution, are obtained as none of the objectives can be improved without affecting others [6], [27], [28].

To solve a multi-objective optimization problem, various methods can be used resulting in an infinite number of Pareto optimal solutions. User preferences are often taken into account to obtain a single suitable solution. A priori articulation of preferences involves stating preferences before the optimization algorithm runs, while a posteriori articulation occurs after the algorithm runs, selecting a solution from the Pareto optimal set. The weighted sum method is commonly used, as it converts multiple objectives into a single scalar function by summing up all weighted objective functions [27]. This approach provides multiple solution points by varying the weights consistently and allows the user to evaluate the best solution by seeing the effect of changing the weight of the objective functions on the total cost.

The output of the optimization problem is the total cost of the system which is divided as follows; manufacturing cost and cost associated with operation cost which includes efficiency of the system (power losses of the system), and in the future, the work will be extended to include the cost associated to the size and weight and the reliability (lifetime and maintenance).

The total cost objective function is solved using the weighted sum method, which means that the objective function $F(\overrightarrow{x})$ is to minimize:

$$F(\overrightarrow{x}) = w_1 F_1(\overrightarrow{x}) + w_2 F_2(\overrightarrow{x}) + ...w_n F_n(\overrightarrow{x})$$

where

$$w_1 + w_2 + ... + w_n = 1$$

and it is the weight of each objective chosen by the user depending on his preference and n is the number of the objectives, and $\overrightarrow{x}$ is the vector of all the variables taken into account.

IV. The Design Specification

The first step of the design process is to determine all of the design specifications. The boost power rate is chosen to be 2 kW, considering that it is the gateway between the battery storage system and the DC/AC inverter, intended for residential applications. The boost will operate in CCM. Moreover, two switches are used instead of a diode and a switch to make it bidirectional. The operating specifications and the design constraints can be found in Table Table I.

A significant consideration in the design of power electronic converters is switching frequency, which also affects overall energy loss and, consequently, the size of the energy storage components, the demands for thermal management thus the total cost of the converter, so it will be the first design parameter to optimize. Besides that, there are other degrees of freedom considered in this work such as the inductor current ripple, the switches' technology, and some inductor design parameters such as the wire diameter and the number of turns, material, and size of the core. This work in this article is a first approach, while the final algorithm of the research will include more degrees of freedom. Such as including the control parameters of the converter. For instance, the bandwidth of the control loops. They can affect the losses and therefore efficiency. Furthermore, they affect the actions/stresses, and therefore the reliability. Which is very important to be considered for the final goal of the research. These parameters can be adjusted in real-time, so it adds some degree of freedom in the design/maintenance of the converter [26].

TABLE I: Design Specifications

Operating Specifications			
Topology		Bi-directional Boost	
P_o		2 kW	
V_{in}		100 V	
V_o		450 V	
ΔV_o		1%	
Design Constraints			
Parameter		**Lower Boundary**	**Upper Boundary**
f_{sw}	kHz	50	200
$\Delta I_{L\|pp}$	p.u.	5%	50%
D_{wire}	mm	0.1	2
N_{turn}		2	100%
Switch Technology		GaN SiC Si	
Core Material		3C81, 3C90, 3C91 3C92, 3C93 3C94, 3C95, 3C96, 3C97, 3F3, 3F5	
Core Size		ETD29, ETD34, ETD39, ETD44 ETD49, ETD54, ETD59	

Despite the wide range of converter topologies, there are three major classes of power components in a converter: magnetics (inductors and/or transformers), capacitors, and semiconductor switches. Taking the degrees of freedom into account, an optimization based on cost and power loss models of these converter components is established, to identify the optimum converter design. The cost and power loss models for each of these components are detailed in the following section.

V. Modeling Approach

In this section, the modeling of the cost of the main components and their power loss is explained in detail. The cost

model is divided into several cost functions to model the cost of each individual component of the converter. However, for some components, the cost value is assumed to be a discrete value while for others the cost is found by a continuous function. In the end, the cost function is the summation of the cost model of every individual component, as below:

$$F_{cost}(\overrightarrow{x}) = F_{switches}(\overrightarrow{x}) + F_{drivers}(\overrightarrow{x}) + F_{cap}(\overrightarrow{x}) + F_{inductor}(\overrightarrow{x}) \quad (1)$$

Furthermore, the power losses in the converter affect its total cost not only its performance. To present the effect of the power losses on the total cost, the total power losses will also be modeled for each component. After that, the total power calculated will be multiplied by the foreseen tariff operation during the expected operating lifetime of the converter. The power losses can be converted to currency and this amount will be added to the manufacturing cost of the converter. Therefore, it is easier to compare what role the efficiency of the converter has on the total cost of the converter. The power losses in the converter are caused mainly by the switches and the passive components such as the capacitor and the inductor. The total power loss function is as follows:

$$F_{Plosses}(\overrightarrow{x}) = F_{switches}(\overrightarrow{x}) + F_{cap}(\overrightarrow{x}) + F_{inductor}(\overrightarrow{x}) \quad (2)$$

A. Semiconductor Transistor

A space of commercial MOSFET transistors of each technology (GaN, SiC, Si) was created to form an initial database, and the essential information was extracted from their data sheets to create the cost and power models.

1) ***Cost model:*** the cost of the switches depends on the technology of the semiconductor as well as the voltage and current ratings of the switch. In this initial stage of the work, the voltage rating is fixed for all of the switches at 800V to be high enough to handle the boost voltage rating, so that, the switches are divided into 2 categories: first one depends on the technology, and then the current ratings. Then, the average cost of all the transistors for the selected technology and current rate was measured, and for each category, check Table II. So as observed from the table a fixed value of cost is given to each category and the cost model of the semiconductors, in this case, is a discrete value. To simplify and understand the problem, we will stick to these 3 technologies of transistors, but the methodology and the algorithm can be valid for more.

TABLE II: Average cost of switches in €

Switch Technology	Current Rate		
	30 - 40 A	40 - 50 A	50 - 60 A
GaN	16.89	20.93	33.07
SiC	14.91	16.59	20.79
Si	8.09	8.0700	13.60

2) ***Power loss model:*** Power losses caused by switches are a significant concern in converters, especially when working at high frequencies [29], [30]. Switching losses and conduction losses are the two components of power loss in semiconductors. Switching losses are determined by various factors such as input current, switching frequency, DC voltage, gate voltage, gate resistance, temperature, and current ripple. Meanwhile, conduction losses are calculated based on switching current and the semiconductor's R_{dson}, which is itself affected by temperature.

Initial data on GaN, SiC, and Si commercial transistor technologies were collected, including data from datasheets on switching losses (E_{on} & E_{off}) and the R_{dson} at various temperature ranges. In cases where datasheets did not provide the necessary information, LTspice simulations were used to extract the required data, if the spice model was not provided the switching energy of these devices is assumed to follow the same trend of other devices from the same technology and current rate category. For the Si MOSFETs, E_{sw} is assumed to be constant against the temperature , as there was no available data on the subject. Using MATLAB, a first-order function was developed to model the switching losses vs temperature and a similar function was developed for R_{dson} vs the temperature. Using these functions, the total power loss caused by switches can be calculated as:

$$P_{cn}(temp, I_{rms}) = I_{rms}^2 R_{dson}(temp) \quad (3)$$

$$I_{rms} = I_{Lavg}\sqrt{D} \quad (4)$$

$$P_{sw}(temp, fsw) = (E_{on}(temp) + E_{off}(temp)) * f_{sw} \quad (5)$$

$$P_{tot}(temp) = P_{sw}(temp) + P_{cn}(temp) \quad (6)$$

B. Capacitor

The output capacitor value in a boost converter is calculated using Eq. 7, where C is the capacitor value, I_o, is the average output current, ΔV_o is the voltage ripple, D is the duty cycle and fsw is the frequency.

$$C = \frac{(I_o D)}{(\Delta V_o f_{sw})} \quad (7)$$

Creating the models of the capacitor was done in several steps, firstly, calculate the value of the capacitor under different frequencies using Eq. 7, was calculated at $50kHz, 100kHz, 150kHz$, and $200kHz$, and keeping the rest of the values fixed. The values of the capacitor will be $15\mu F, 7.5\mu F, 5\mu F$ and $3.6\mu F$ respectively. After that, 5 commercial film capacitors were chosen for each value from different manufacturers, these capacitors have the same DC voltage rating (800V), so the peak voltage of the converter does not exceed their rated DC voltage. The information saved in the database was the cost per unit, the volume of the capacitor, and the ESR value.

Film capacitors have a high current capability, and low ESR and ESL. They were chosen because the required capacitor values are not large and they are used for filtering. In future work, mixing different technologies can be considered to see how this can improve the cost, the losses, and the volume of the system.

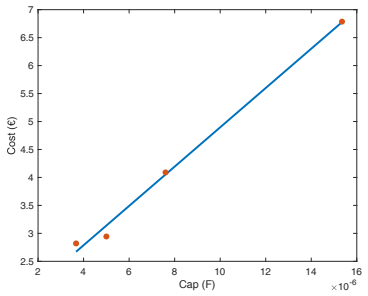

Fig. 3: Capacitor cost function

1) ***Cost model****:* the cost model for the capacitors differs from the switches one as capacitors have a continuous cost function due to the various interacting variables such as frequency, voltage, current, ripple values, and the number and type of capacitors used in combination. The value of capacitors is directly dependent on frequency, making it a function of frequency. To determine the cost, grouped commercial capacitors were analyzed and average cost was calculated for each group. A linear function was then created between the capacitor cost and its value, and it can be noted as frequency increases, the value and cost of the capacitor decreases. The approximated linear cost function of the capacitor Vs its value is shown below in Fig. 3.

2) ***Power loss model****:* The power losses in a capacitor are calculated as follows.

$$P_{cap} = I_{c|rms}^2 * ESR_{|rms} \tag{8}$$

where ESR is the equivalent series resistance of the capacitor, and $I_{c|rms}$ is the RMS capacitor current. The RMS capacitor current is calculated based on the converter topology, thus for a boost converter, the expression is as follows.

$$I_{c|rms} = I_{Lavg} * \sqrt{\left(D + \frac{\Delta I_L|\ rms^2}{12}\right)(1-D)} \tag{9}$$

The ESR, in turn, depends on the capacitive reactance, and the dissipation factor, DF, also called the tangent of the loss angle $tan\delta$. But this value was not provided in some datasheets. Therefore, from observing the data sheets of capacitors, it seems that the ESR of a capacitor decreases when the value of the capacitor increases. The losses from the capacitors can be expressed as a function of their value, which is a function of the frequency voltage ripple and, output voltage and duty cycle, but since now, only the frequency is considered as a degree of freedom, then the ESR will be affected by changing the frequency. As well, the capacitor loss is a function of the current ripple which is considered as a degree of freedom too.

To check those parallel combinations might be a better solution for the converter, a function of $C_{parallel} = C_{Total}/N$, and N will be a degree of freedom for the optimizer to find. Then the cost will be calculated by the cost of $C_{parallel} * N$, and the losses will be $ESR(C_{parallel})/N * I_{rms}^2$. It might increase the cost and the volume but losses will be reduced.

C. Inductor

By defining the boost converter's operation parameters, such as the switching frequency range, and the current waveform (average and ripple range), the corresponding inductance ranges can be calculated, which are calculated by

$$L = \frac{V_{in}D}{I_{pp|HF}f_{sw}} \tag{10}$$

Where L is the inductor value, V_{in} is the boost input voltage, D is the duty cycle, and f_{sw} is the switching frequency. $I_{pp|HF}$ is the current high-frequency ripple, and it is calculated as follows

$$I_{pp|HF} = I_{Lavg} * \Delta I_{L|pp} \tag{11}$$

where $I_{L|pp}$ is the p.u. current ripple and I_{Lavg} is the average current value. Depending on the converter topology, the HF and LF current components can be calculated as a function of the current ripple. Specifically for a boost converter, more details about current measurement can be found in [31], [32]

1) ***Cost model****:* Inductors' hardware cost is more complicated than the capacitor and it can be divided into three parts: design cost, material cost, and manufacturing cost. Material cost depends on the power density, windings (round, Litz, plate, planar) and heat transfer/ airflow/ fans, and frequency: which affects materials cost by decreasing if frequency increases. manufacturing cost depends on the type of winding and the number of samples. This part of the work is still in progress.

2) ***Power loss model****:* Power loss in an inductor is divided mainly into copper losses, both Low Frequency (LF) and High Frequency (HF) components, and core losses. Each of the latter loss components is discussed in detail in this section.

Core Losses

The power losses in a magnetic core are a function of several parameters, such as the switching frequency, current ripple, magnetic core material, core size, and winding number of turns, $P_{core}(f_{sw}, \Delta I_{pp|HF}, Material, Size, N)$. For the analytical approach, hereby in context, the well-known empirical equation, known as the standard Steinmetz Equation (SE) [33], is used:

$$P_{core} = c * f_{sw}^x * (B_{ac|HF})^y * V_e \tag{12}$$

where c, x, and y are the Steinmetz coefficients which are a function of the core material and the switching frequency. V_e is the core volume, $B_{ac|HF}$ is the AC magnetic flux density, more details can be found in [33]–[35].

Copper Losses

The copper losses are a function of several parameters, such as the current ripple, core size, wire diameter, and winding number of turns, $P_{copper}(\Delta I_{pp|HF}, Size, Diameter, N)$. Copper losses are divided into LF (or DC component) and HF (or AC component) losses. The low-frequency losses are calculated using the DC winding resistance, while the high-frequency losses (represent skin and proximity effects) are calculated using Dowell's formulae and procedure. Detailed

derivation can be found in [36], [37]. However, the final equation will be

$$P_{copper} = \left(I_{rms|LF}^2 + I_{Lavg}^2\right) R_{dc} + \left(I_{rms|HF}^2\right) R_{ac} \quad (13)$$

So the total power losses of an inductor are the sum of the copper and core losses.

$$P_{L_{tot}} = P_{copper} + P_{core} \quad (14)$$

D. Drivers

The drivers' cost model is not straightforward because there are many technologies. To simplify it in this stage, a specific driving method was used and the cost of the drivers is taken as a function of switch technology. To simplify this part and to reduce the cost the bootstrapping drivers were chosen at this point. So, a set of drivers were collected for each technology besides the diodes and the capacitors that can be used. After choosing the specific technology of transistor, the cost function will check and take the average cost of the drivers that work with that technology. As shown in Table III. However, the power losses caused by drivers are not considered at this stage, as they can be neglected when compared to the rest of the converter's main components.

TABLE III: Drivers Database

Driver	Transistors	Price
NCP51820AMNTWG	GaN Si	3.03
1EDB9275FXUMA1	GaN Si SiC	2.06
IR2110STRPBF	Si	3.78
2ED2104S06F	SiC Si	1.41
1EDN6550BXTSA1	GaN SiC	1.34

VI. Optimization Results

In this section, some test results are presented. The tests are done for switches with the highest current rate, and three different cases are presented. Note that the chromosome of the genetic algorithm has 8 genes which are: 1. the current ripple 2. the switching frequency 3. the number of turns for the inductor wire 4. the diameter of the inductor wire 5. the core material of the inductor 6. the core size of the inductor 7. the semiconductor 8. number of capacitors in parallel.

A. Case One

In this case, the cost function has higher importance to optimize than the losses, but as well the losses are still considered in the optimization. The weight for the cost function is 0.9, and 0.1 for the power losses. The results are shown in Table IV.

B. Case Two

In this case, the power loss function has higher importance to optimize than the cost. The weight for the cost function is 0.1, and 0.9 for the power losses. The results are shown in Table V.

TABLE IV: Case One

Chromosome	
$\Delta I_{L\|pp}$	16%
f_{sw}	135 kHz
N_{turn}	60
D_{wire}	1.5mm
Core Material	3F5
Core size	ETD49
Switch Tech	SiC - UF3C065040T3S
N_{cap}	1
Solutions	
P_{sw}	40.94 W
P_{Ind}	27.69 W
P_{Cap}	0.79 W
C	5.6 μF
L	180 μH
Driver	1EDN6550BXTSA1
Switch Cost	28.18 €
Driver Cost	1.34 €
Capacitor Cost	3.38 €

TABLE V: Case Two

Chromosome	
$\Delta I_{L\|pp}$	31%
f_{sw}	50 kHz
N_{turn}	44
D_{wire}	2mm
Core Material	3F5
Core size	ETD59
Switch Tech	GaN - LMG3422R030RQZT
N_{cap}	4
Solutions	
P_{sw}	5.68 W
P_{Ind}	18.92 W
P_{Cap}	0.22 W
C	15 μF
L	232 μH
Driver	1EDN6550BXTSA1
Switch Cost	44 €
Driver Cost	1.34 €
Capacitor Cost	10.9 €

TABLE VI: Case Three

Chromosome	
$\Delta I_{L\|pp}$	31%
f_{sw}	55 kHz
N_{turn}	56
D_{wire}	17.5mm
Core Material	3F5
Core size	ETD54
Switch Tech	SiC - UF3C065040T3S
N_{cap}	2
Solutions	
P_{sw}	16.94 W
P_{Ind}	21,86 W
P_{Cap}	0.37 W
C	13.9 μF
L	228 μH
Driver	1EDN6550BXTSA1
Switch Cost	28.18 €
Driver Cost	1.34 €
Capacitor Cost	7.67 €

C. Case Three

In this case, both functions are equal in importance and the weight for both is 0.5. The results are shown in Table VI.

Upon comparison of the three cases, it is evident that the

first case prioritized selecting components with minimum cost over minimizing power losses. The frequency was chosen to be higher to reduce capacitor cost, with only one capacitor being used. The program opted for a switch type with low cost and low power losses. In contrast, the second case placed a higher importance on minimizing power losses, selecting GaN as the switch with the lowest power losses, albeit with a higher cost. The frequency was set at 50 kHz to minimize switching losses, and four capacitors were used in parallel to reduce capacitor losses. Additionally, the inductor losses were lower in the second case than in the first. The third case represents a design that falls between the first two, check Table VI. Once an optimal design is obtained, it is essential to verify it by conducting simulations and creating a hardware prototype.

VII. Conclusion

This paper proposes a multi-objective optimization algorithm that optimizes the cost and power losses to improve the efficiency of dc-dc converters. The algorithm is applied to find the optimal designs of bidirectional boost converters that are connected to the battery and DC/AC inverter in nanogrids. Analytical models of converter components, including inductors, capacitors, and semiconductors, are used to provide the basis for optimization. The genetic algorithm is used due to its ability to solve mixed-integer and nonlinear optimization problems. The weighted sum method is applied to obtain a single solution that allows users to indicate their preferences. Three different cases with varying weights demonstrate the algorithm's ability to provide solutions based on the objective function's weight. Future work will include more objective functions such as reliability, weight, and size of the converter, and a multi-objective optimization that includes a mission profile. This paper is the first step towards creating a global optimization tool that translates all objective functions into a common framework, which will require considering more degrees of freedom..

References

[1] R. Lasseter, "MicroGrids," in *2002 IEEE Power Engineering Society Winter Meeting. Conference Proceedings (Cat. No.02CH37309)*. IEEE.

[2] X. Wang, J. Guerrero, F. Blaabjerg, and Z. Chen, "A review of power electronics based microgrids," *Journal of power electronics*, vol. 12, pp. 181–192, 01 2012.

[3] W. Wu, H. Wang, Y. Liu, M. Huang, and F. Blaabjerg, "A dual-buck–boost AC/DC converter for DC nanogrid with three terminal outputs," *IEEE Transactions on Industrial Electronics*, vol. 64, no. 1, pp. 295–299, jan 2017.

[4] K. R. Naik, B. Rajpathak, A. Mitra, and M. Kolhe, "A review of nanogrid technologies for forming reliable residential grid," in *2020 IEEE First International Conference on Smart Technologies for Power, Energy and Control (STPEC)*. IEEE, sep 2020.

[5] D. Burmester, R. Rayudu, W. Seah, and D. Akinyele, "A review of nanogrid topologies and technologies," *Renewable and Sustainable Energy Reviews*, vol. 67, pp. 760–775, jan 2017.

[6] G. Adinolfi, G. Graditi, P. Siano, and A. Piccolo, "Multiobjective optimal design of photovoltaic synchronous boost converters assessing efficiency, reliability, and cost savings," *IEEE Transactions on Industrial Informatics*, vol. 11, no. 5, pp. 1038–1048, oct 2015.

[7] F. Tian, D. B. Cobaleda, and W. Martinez, "Artificial-intelligence based dc-dc converter efficiency modelling and parameters optimization," in *2022 24th European Conference on Power Electronics and Applications (EPE'22 ECCE Europe)*, 2022, pp. 1–7.

[8] J. He, A. Sangwongwanich, Y. Yang, and F. Iannuzzo, "Lifetime evaluation of power modules for three-level 1500-v photovoltaic inverters," in *2020 IEEE Applied Power Electronics Conference and Exposition (APEC)*. IEEE, mar 2020.

[9] H. Du, P. D. Reigosa, F. Iannuzzo, and L. Ceccarelli, "Impact of the case temperature on the reliability of SiC MOSFETs under repetitive short circuit tests," in *2019 IEEE Applied Power Electronics Conference and Exposition (APEC)*. IEEE, mar 2019.

[10] H. Wang, F. Iannuzzo, A. S. Bahman, K. Zhang, P. Xue, Y. Zhang, B. Yao, Z. Shen, A. Sangwongwanich, I. Vernica, Y. Song, S. Sahoo, and F. Blaabjerg, "Application-oriented reliability testing of power electronic components and converters," *IEEE Power Electronics Magazine*, vol. 9, no. 4, pp. 22–31, dec 2022.

[11] J. He, A. Sangwongwanich, Y. Yang, K. Zhang, and F. Iannuzzo, "Design for reliability of SiC-MOSFET-based 1500-v PV inverters with variable gate resistance," *IEEE Transactions on Industry Applications*, vol. 58, no. 5, pp. 6485–6495, sep 2022.

[12] M. Mirjafari and R. S. Balog, "Multi-objective design optimization of renewable energy system inverters using a descriptive language for the components," in *2011 Twenty-Sixth Annual IEEE Applied Power Electronics Conference and Exposition (APEC)*. IEEE, mar 2011.

[13] B. K. Bose, "Artificial intelligence techniques: How can it solve problems in power electronics?: An advancing frontier," *IEEE Power Electronics Magazine*, vol. 7, no. 4, pp. 19–27, dec 2020.

[14] P. Qashqai, H. Vahedi, and K. Al-Haddad, "Applications of artifical intelligence in power electronics," in *2019 IEEE 28th International Symposium on Industrial Electronics (ISIE)*. IEEE, jun 2019.

[15] S. Zhao, F. Blaabjerg, and H. Wang, "An overview of artificial intelligence applications for power electronics," *IEEE Transactions on Power Electronics*, vol. 36, no. 4, pp. 4633–4658, apr 2021.

[16] Q. Wang and S. Niu, "Design, modeling, and control of a novel hybrid-excited flux-bidirectional-modulated generator-based wind power generation system," *IEEE Transactions on Power Electronics*, vol. 33, no. 4, pp. 3086–3096, apr 2018.

[17] S. Lyden and M. E. Haque, "A simulated annealing global maximum power point tracking approach for PV modules under partial shading conditions," *IEEE Transactions on Power Electronics*, vol. 31, no. 6, pp. 4171–4181, jun 2016.

[18] S. Busquets-Monge, G. Soremekun, E. Hertz, C. Crebier, S. Ragon, D. Boroyevich, Z. Gurdal, M. Arpilliere, and D. Lindner, "Power converter design optimization," *IEEE Industry Applications Magazine*, vol. 10, no. 1, pp. 32–39, jan 2004.

[19] J. Zhang, Y. Shi, and Z. hui Zhan, "Power electronic circuits design: A particle swarm optimization approach," in *Asia-Pacific Conference on Simulated Evolution and Learning*, 2008.

[20] L. L. Jiang, D. L. Maskell, and J. C. Patra, "A novel ant colony optimization-based maximum power point tracking for photovoltaic systems under partially shaded conditions," *Energy and Buildings*, vol. 58, pp. 227–236, mar 2013.

[21] X. Li, X. Zhang, F. Lin, and F. Blaabjerg, "Artificial-intelligence-based design for circuit parameters of power converters," *IEEE Transactions on Industrial Electronics*, vol. 69, no. 11, pp. 11 144–11 155, nov 2022.

[22] K. Deb, A. Pratap, S. Agarwal, and T. Meyarivan, "A fast and elitist multiobjective genetic algorithm: NSGA-II," *IEEE Transactions on Evolutionary Computation*, vol. 6, no. 2, pp. 182–197, apr 2002.

[23] X. Huang, X. Zhang, and X. Li, "Multi-objective optimization for smaller, efficient and better performed design of buck-boost converters," in *2020 IEEE 11th International Symposium on Power Electronics for Distributed Generation Systems (PEDG)*. IEEE, sep 2020.

[24] D. Malyna, J. Duarte, M. Hendrix, and F. van Horck, "Multi-objective optimization of power converters using genetic algorithms," in *International Symposium on Power Electronics, Electrical Drives, Automation and Motion, 2006. SPEEDAM 2006.* IEEE.

[25] J. Biela, S. Waffler, and J. Kolar, "Mission profile optimized modularization of hybrid vehicle DC/DC converter systems," in *2009 IEEE 6th International Power Electronics and Motion Control Conference*. IEEE, may 2009.

[26] J. García, C. González-Morán, P. García, and P. Arboleya, "A methodology for the assessment of efficiency in systems under transient conditions: Case study for hybrid storage systems in elevators," in *Springer Optimization and Its Applications*. Springer International Publishing, 2022, pp. 253–284.

[27] R. T. Marler and J. S. Arora, "The weighted sum method for multi-objective optimization: new insights," *Structural and Multidisciplinary Optimization*, vol. 41, no. 6, pp. 853–862, dec 2009.

[28] S. Waffler, M. Preindl, and J. W. Kolar, "Multi-objective optimization and comparative evaluation of si soft-switched and SiC hard-switched automotive DC-DC converters," in *2009 35th Annual Conference of IEEE Industrial Electronics*. IEEE, nov 2009.

[29] R. A. Mdanat, R. Georgious, J. Garcia, G. D. Donato, and F. G. Capponi, "Characterization of GaN HEMT transistors for DC/DC converters in transportation applications," in *2020 IEEE Vehicle Power and Propulsion Conference (VPPC)*. IEEE, nov 2020.

[30] R. A. Mdanat, S. Saeed, R. Georgious, and J. Garcia, "Analytical power loss model for GaN transistors," in *2021 IEEE Vehicle Power and Propulsion Conference (VPPC)*. IEEE, oct 2021.

[31] M. Kamil, "Switch mode power supply (smps) topologies - microchip technology," 2007. [Online]. Available: https://ww1.microchip.com/downloads/en/appnotes/01114a.pdf

[32] A. Bersani, "Switch mode power supply (smps) topologies (part ii), an1207," 2009. [Online]. Available: https://ww1.microchip.com/downloads/en/Appnotes/01207B.pdf

[33] C. P. Steinmetz, "On the law of hysteresis," *Transactions of the American Institute of Electrical Engineers*, vol. IX, no. 1, pp. 1–64, jan 1892.

[34] S. Saeed, J. Garcia, and R. Georgious, "Dual-active-bridge isolated DC–DC converter with variable inductor for wide load range operation," *IEEE Transactions on Power Electronics*, vol. 36, no. 7, pp. 8028–8043, jul 2021.

[35] S. Saeed, J. Garcia, M. S. Perdigao, V. S. Costa, B. Baptista, and A. M. S. Mendes, "Improved inductance calculation in variable power inductors by adjustment of the reluctance model through magnetic path analysis," *IEEE Transactions on Industry Applications*, vol. 57, no. 2, pp. 1572–1587, mar 2021.

[36] P. L. Dowell, "Effects of eddy currents in transformer windings," 1966.

[37] S. S. H. Gerges, "Contributions for the design operation and control of dab bidirectional converters based on variable magnetic elements," Ph.D. dissertation, University of Oviedo, Jun 2020. [Online]. Available: http://hdl.handle.net/10651/57687